

Corrosion Protection of Synthetic Bronze Patina

K. Marušić[†], H. Otmačić-Ćurković, H. Takenouti,* A. D. Mance, and E. Stupnišek-Lisac

Faculty of Chemical Engineering and Technology, University of Zagreb, Croatia
kmarusic@fkit.hr, hotmac@fkit.hr, admance@fkit.hr, elisac@fkit.hr

*Laboratoire Interfaces et Systèmes Electrochimiques (LISE), CNRS,
Université Pierre et Marie Curie, Paris, France
ht@ccr.jussieu.fr

Original scientific paper
Received: October 15, 2006
Accepted: December 13, 2006

Bronze artifacts are generally covered with green or blue coloured corrosion products called patina, which not only enhances the good appearance of the bronze, but also helps to protect it. Because of the increased air pollution and acid rain the large collection of statues and works of art made from bronze exposed in the urban environment could be damaged. The increase of air pollution damages also archaeological bronze objects exposed or stored in a museum. This is why it is necessary to find ways to improve the protection that the patina gives to bronze. In order to preserve metal works from the aggressive atmosphere, organic inhibitors are often employed. The inhibiting effects of two imidazole derivatives (4-methyl-1-phenylimidazole and 4-methyl-1-(*p*-tolyl)imidazole) on artificial patina were examined. The results of these investigations have shown that both inhibitors studied improve the protective properties of bronze patina in simulated urban acid rains.

Key words:

Archeological artefact, imidazole, artificial patina, electrochemical impedance spectroscopy, energy dispersive X-ray spectroscopy

Introduction

When exposed to their environment, bronze objects, undergo a corrosion process, leading to the formation of a protective layer of corrosion products on their surface.¹ This kind of patina is called *natural patina* and it forms spontaneously. Depending on the environment it is exposed to, the patina has a specific structure.² The second type of patina is *synthetic* or *artificial patina* with defined chemical composition that can be formed in the laboratory allowing appropriate accelerated surface treatment of bronze.^{3,4}

Synthetic patina with a similar composition as the natural patina is used for the present investigations. There are two electrochemical methods for making artificial patina; potentiostatic (under potential control) and galvanostatic (under current regulation). The patina formation was carried out in a sulphate/carbonate solution to mimic an urban atmospheric conditions.

Because of an increase of air pollution leading to acid rainfall, the bronze and patina in urban atmospheres are being destroyed. Therefore, a similar solution to the patina formation medium, but acidified to pH 5, is used for the corrosion test solution corresponding to acid rain in an urban zone. Previous investigations^{5–11} have shown that the environ-

mentally friendly imidazole derivatives are good copper corrosion inhibitors in different media. It is reasonable to expect then that these compounds are also valid for other bronzes, if they showed a marked protective effect for these two different copper alloys

Experimental conditions

To obtain a representative patina in a short period, the patina was synthesised by two different electrochemical methods, on two different bronzes: Cu-8Sn-14Pb (B66 bronze) and Cu-6Sn. The composition of these alloys is given in Table 1.

The concentration was normalized so that the sum of the all elements analyzed by EDS (Energy dispersive X-ray spectroscopy) is 100 %. This is also the case for all other EDS results.

Table 1 – Composition of the B66 and Cu-6Sn bronze in atomic %

	Sn	Pb	Ni	Zn	Fe	Sb	P	Cu
B66	7.91	13.60	0.59	0.52	0.22	0.15	0.02	76.99
Cu-6Sn	6.10	0.01	0	0.10	0.02	0	0.11	93.66

The concentration normalized to 100 % for the total of elements analyzed.

[†]Corresponding author

Cu-6Sn bronze was the composition representative of the Transylvanian archaeological patina of the last Neolithic to Roman period.¹² Bronze B66 containing lead as an alloy element is, in contrast, selected as the representative of bronze coins found in Morocco for the Post-Roman era.¹³ Therefore, the composition of two bronzes correspond to that of the cultural heritage, rather than bronze statues exposed in the urban area. The aim of this paper is to discover whether the anticorrosion effect of imidazole compounds used are valid for two different compositions, one a Cu-Sn binary alloy and the other Cu-Sn-Pb ternary alloy.

Patina was synthesized, on both bronzes, in an aerated solution composed of $\gamma = 0.2 \text{ g L}^{-1} \text{ Na}_2\text{SO}_4 + \gamma = 0.2 \text{ g L}^{-1} \text{ NaHCO}_3$ at 30 °C. The pH of this solution, as prepared was ca 8.5. This solution is expected to produce a patina characteristic for the urban environment. The SO_4^{2-} ions are one of the main pollutants in urban atmosphere due to the industrial activity and the car exhaust emission.

Patina on the B66 bronze (Pb containing the bronze above) was synthesised during 24 h under a constant anodic current density $j = 30 \mu\text{A cm}^{-2}$.

The patina on the Cu-6Sn bronze was synthesised under potential regulation:

- During 60 s at -0.2 V vs. to the initial open circuit potential, that varies substantially from one specimen to another.

- The potential of the open circuit becomes reproducible and is equal to -0.05 V vs. SCE .

- Patina formation during the next 48 h at 0.09 V vs. SCE .

- Second step patina formation during another 48 h at 0.07 V vs. SCE .

This procedure introduced later in the present work, though more complicated than the current regulation method, allowed patina formation of six electrodes simultaneously. The first step is introduced for two reasons; to increase the reproducibility and to avoid the formation of pits at the electrode surface. This step allows the reduction of a native oxide layer, formed during the time separating between the moment when the electrode was polished, and the time when it was dipped into the patina formation solution. The overall current density is lower, compared to the patina formation at a constant current. Consequently, so is the thickness of the patina layer for the same polarization period. A slow patina formation allowed, in contrast, the structure closer to the natural patina.¹⁴ This process is therefore well adapted to compare the inhibiting effect of a few compounds simultaneously.

The morphology and crystallographic structure of artificially obtained patina were examined with Scanning Electron Microscopy (SEM) and X-ray

Elemental Energy Dispersion Spectroscopy (EDS) analyses. SEM studies were performed with a Leica Stereoscan 440 coupled with EDS elemental semi-quantitative analyses (Princeton Gamma-Tech, Inc.) at 20 keV.

The protective characteristics of patinated bronze with and without the presence of inhibitors were investigated by electrochemical impedance spectroscopy (EIS). Measurements were performed using EG&G potentiostat/galvanostat Model 263A and Frequency Response Detector 1025 that were controlled with Power-Sine software. The EIS measurements were carried out in $\gamma = 0.2 \text{ g L}^{-1} \text{ Na}_2\text{SO}_4 + \gamma = 0.2 \text{ g L}^{-1} \text{ NaHCO}_3$ acidified to pH 5 by addition of a dilute sulphuric acid at room temperature without regulation. The corrosion test solution is at the thermodynamic equilibrium to ambient air.

The investigated corrosion inhibitors were: 4-methyl-1-phenylimidazole (PMI at concentration $c = 5 \text{ mmol L}^{-1}$) and 4-methyl-1-(*p*-tolyl)imidazole (TMI at $c = 1 \text{ mmol L}^{-1}$). The inhibitor concentration was selected according to our former work on the copper electrode for Cu-Sn-Pb alloy.^{10–11}

Results and discussion

SEM observation and EDS analyses

The artificial patina formed by electrochemical synthesis was dried at room temperature and observed by SEM.

Fig. 1 and 2 show the structure of patina on the surface of B66 and Cu-6Sn bronze. The SEM pictures show different structures of patina layers. The B66 bronze has three layers (Fig. 1, point 1, 2, 3). EDS analyses were carried out on these layers and the results are summarized in Table 2.



Fig. 1 – SEM image of the B66 bronze covered with a synthetic patina formed by galvanostatic method

Table 2 – The elemental composition in atomic % of the B66 and Cu-6Sn bronze patinas at three different positions

	Position	Cu	S	O	Sn
B66 bronze	1	33.1	2.6	64.2	0.1
	2	35.2	1.5	63.2	0.1
	3	26.4	2.9	57.8	12.9
Cu-6Sn	1	20.1	0.5	79.4	0
	2	35.6	1.1	63.3	0
	3	51.6	0.1	47.9	0.4

The outer layer of the B66 bronze patina (Point 1. in Fig.1.) is rich in copper (33 %) and oxygen (64 %) and contains some quantity of sulphur (3 %) while the content of tin is negligible. The carbon-content was clearly observed, but not analysed because the EDS is insufficiently accurate for this element. Copper is soluble and by dissolution – precipitation mechanism, it forms patina with granular structure (point 1 in Fig. 1) which consists of $(\text{Cu}_4(\text{OH})_6\text{SO}_4)$ and $\text{Cu}_2(\text{CO}_3)(\text{OH})_2$. This interpretation is essentially supported by the Raman spectroscopy analyses reported elsewhere.^{4,17}

The intermediate layer (point 2. in Fig.1.) is also rich in copper and oxygen but has a very different, smooth structure which indicates that the intermediate layer contains cuprite (Cu_2O), characterized by a reddish colour.

The composition of the inner layer (point 3. in Fig.1.) shows an enrichment in tin (12 %) and decrease in copper content (26 %). It is important to note that the selective dissolution of copper from the bronze matrix is one of the main features of bronze corrosion and patina formation. This process is known as decuprification. This is the same process found on newly patinated bronze as well as on archaeological bronzes².

The Cu-6Sn bronze also has three layers (Fig. 2, points 1, 2, and 3). EDS analyses were also carried out on these layers of the Cu-6Sn bronze patina and they are summarized in the Table 2.

Layer 1 on the Cu-6Sn bronze (Point 1 on Fig. 2) contains a significant amount of oxygen (79 %) and a small amount of sulphur (0.5 %). This means that this layer is formed of copper-oxide, with a small amount of copper-sulphate.

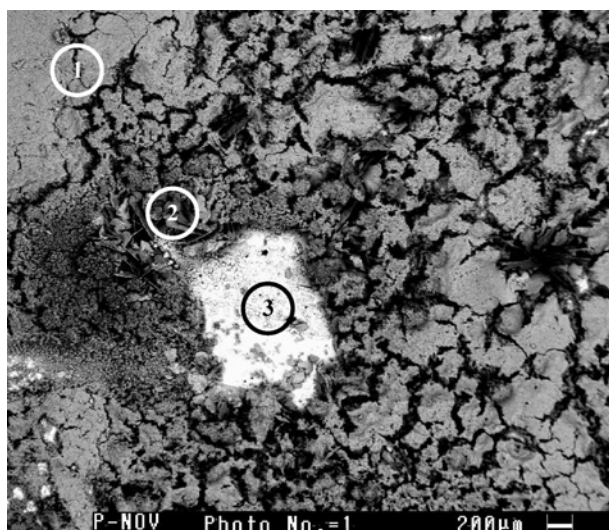


Fig. 2 – SEM image of the Cu-6Sn bronze covered with artificial patina formed under potential regulation

The crystalline structure that can be observed on the SEM picture as layer 2 (point 2, Fig. 2) contains a greater amount of copper (36 %) and sulphur (1. %) than layer 1. Thus, it can be assumed that in this part of the bronze copper-sulphate crystals are the main corrosion product (Fig. 2). This layer is rough, and probably the laser beam collected also the inner layer formed essentially copper oxide. But, the colour of this part is in favour of copper salt.

Layer 3 (point 3, Fig. 2) contains mostly copper (52 %) and oxygen (48 %) which form copper-oxide (Cu_2O) (Fig. 4) like the intermediary layer on the B66 bronze. It is not completely excluded that there is an inner most layer rich in tin oxide, but we did not succeed in reaching this stratum.

EIS measurements

Electrochemical impedance spectroscopy (EIS) was applied on both bronzes covered with artificial patina in order to investigate the protective effect of two imidazole derivatives; 4-methyl-1-phenylimidazole (PMI) and 4-methyl-1-(*p*-tolyl)imidazole (TMI). After the impedance measurements in the sulphate/carbonate solution, the electrodes were immersed in the sulphate / carbonate solution containing one of the studied inhibitors. The influence of PMI on the EIS spectra on the bronze B66 covered with patina is presented in Fig. 3a and that of TMI in Fig. 3b. Fig. 4a illustrates the effect of PMI on the Cu-6Sn bronze with artificial patina and Fig. 4b that of TMI. These spectra were collected after one hour of immersion in the corrosion test solution. First, the EIS was collected in the solution without inhibitor, then with the inhibitor added to the corrosion test solution.

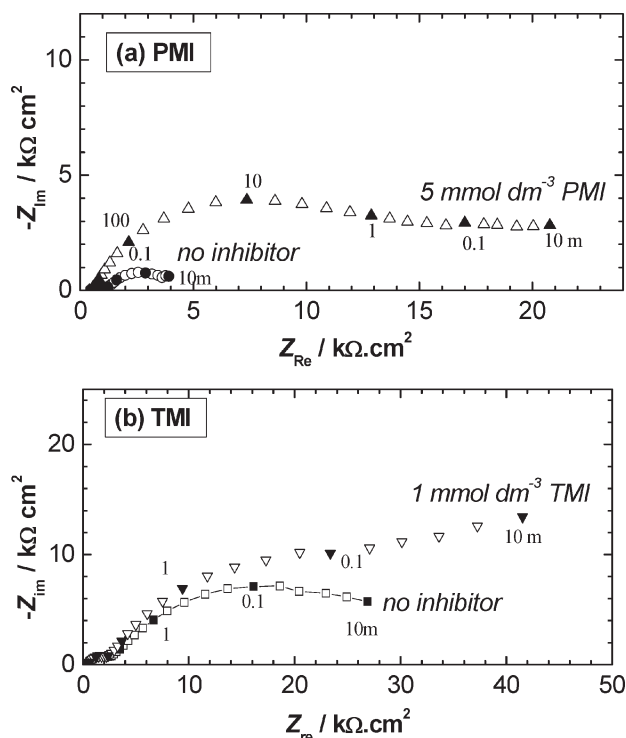


Fig. 3 – EIS spectra of the B66 bronze covered with an artificial patina in sulphate/carbonate solution a) with and without the addition of 5 mmol L^{-1} PMI; b) with and without the addition of 1 mmol L^{-1} TMI

Though not clearly seen for many diagrams, there are three capacitive loops involved in the impedance spectra. Therefore, the equivalent electrical circuit depicted in Fig. 5 was used to carry out the parameters fitting with a simplex method.

The R_f - C_f circuit, the contribution of which will be revealed in the high frequency domain, corresponds to the capacitance and resistance of the surface film, likely the oxide layer which is too thin to be observed by SEM picture. The C_f is related to the dielectric property of this layer whereas R_f denotes an ionic leakage through this layer. The medium frequency circuit R_t - C_d corresponds to the charge transfer resistance and the double layer capacitance. The low frequency loop represented by the R_F - C_F circuit is allocated to faradic resistance and faradic capacitance,¹² implying the patina layer and eventually oxidation – reduction reaction induced by the dissolved oxygen.

Table 3 summarizes the results of the regression calculation.

The results relative to the blank test, that is the EIS measured before addition of the inhibitor scattered significantly. This phenomenon was explained by the formation of a native oxide layer between the moment when the patina formation was made, and the effect of imidazole compounds was evaluated.¹² When recorded successively the impedance

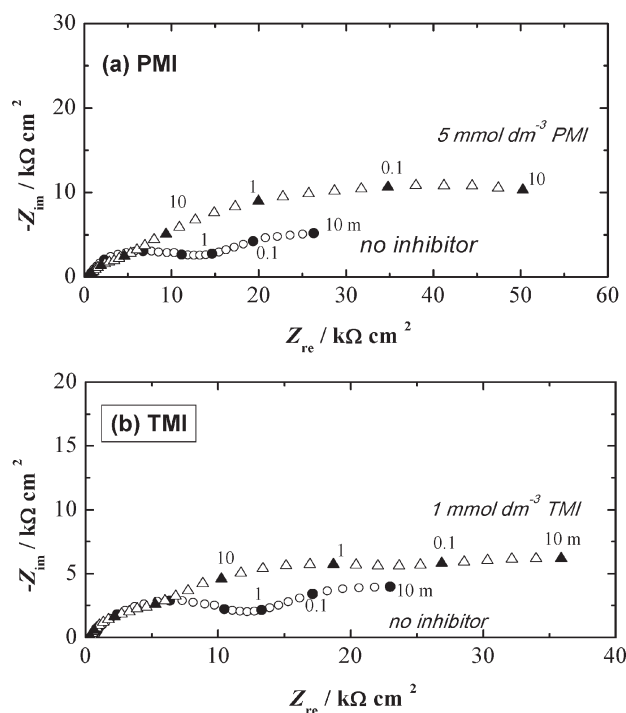


Fig. 4 – EIS spectra of the patinated Cu-6Sn bronze in sulphate/carbonate solution a) with and without the addition of 5 mmol L^{-1} PMI; b) with and without the addition of 1 mmol L^{-1} TMI

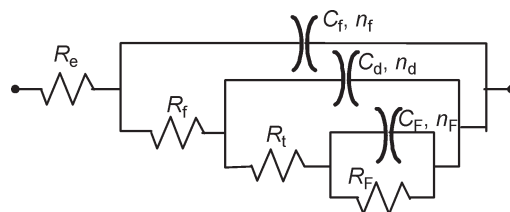


Fig. 5 – Equivalent circuit used for fitting EIS data

spectra in the corrosion test solution without inhibitor, the low frequency limit of the impedance decreased at the initial period corresponding to the dissolution of the native oxide layer, then increased with time corresponding to the formation of another oxide layer at the bronze surface.

The value of C_f is located between 0.1 and $1 \mu\text{F cm}^{-2}$, which is in agreement with the formation of a thin surface film. This capacitance may correspond likely to the oxide film located between the substrate bronze and the patina layer. In this hypothesis, the permittivity of many oxides is close to 10, and then if the model of planer capacitance is applied, the thickness of the oxide film is evaluated to be $\delta = 10$ to 100 nm . This value validates the hypothesis on the origin of the high frequency capacitive loop. In the solution containing the PMI, R_f of the B66 bronze with patina layer is much higher than in the uninhibited solution (Sample 1). Also, the increase of C_f is observed which is in agreement

Table 3 – EIS data of the bronze electrodes covered with artificial patina in sulphate / carbonate solution with and without addition of the inhibitors examined

Bronze	B66				Cu-6Sn			
	Blank	PMI	Blank	TMI	Blank	PMI	Blank	TMI
R_p , $k\Omega\text{ cm}^2$	0.613	9.29	2.11	2.11	5.66	3.92	7.27	4.60
C_p , mF cm^{-2}	0.11	0.81	0.12	0.13	0.05	0.07	0.07	0.04
n_f	0.63	0.70	0.73	0.74	0.80	0.75	0.69	0.71
R_t , $k\Omega\text{ cm}^2$	3.0	5.2	28.0	30.9	8.2	35.1	5.3	23.5
C_d , mF cm^{-2}	221	24	60	19	0.7	5.6	1.0	3.2
n_d	0.59	0.50	0.59	0.67	0.52	0.53	0.61	0.52
R_F , $k\Omega\text{ cm}^2$	1.9	10.6	2.9	25.0	22.1	33.5	16.5	18.6
C_F , mF cm^{-2}	41	0.49	4.5	0.51	0.36	0.36	0.38	0.62
n_F	0.97	0.51	0.92	0.80	0.50	0.51	0.53	0.58

Blank: Data from the EIS determined before inhibitor addition in the solution.

with the transformation of the surface film to a new and a thin protective oxide layer. In contrast, R_f and C_f of the B66 sample immersed in the TMI containing the solution are similar to those observed in the uninhibited solution. The TMI modifies little the oxide layer. R_t value in both studied corrosion inhibitors is much higher than that in the uninhibited solution. That is, these compounds hinder markedly the corrosion kinetics.

The R_F - C_F loop corresponds, as mentioned above, to a redox process involving corrosion products or dissolved oxygen. From the data in Table 3, it can be seen that this process is slowed down in the presence of both inhibitors. The formation of a complex with the patina and the inhibitor may stabilize the patina layer. This is an interesting feature since the imidazole not only hinders the corrosion rate of the substrate bronze, but also slows down the degradation of the patina layer with time.

For Cu-6Sn bronze, the addition of both PMI and TMI modify scarcely the value R_f and C_f . Therefore, these molecules do not modify substantially the surface oxide film. In contrast, R_t increases significantly in the presence of both substances, therefore they slow down dramatically the corrosion process. This is also true for R_F . In other words, PMI and TMI allow first the inhibition of bronze corrosion and second the stabilization of the patina layer leading to the protection of the substrate bronze.

Figure 6 illustrates, for example, the time change of the impedance spectrum of B66 bronze

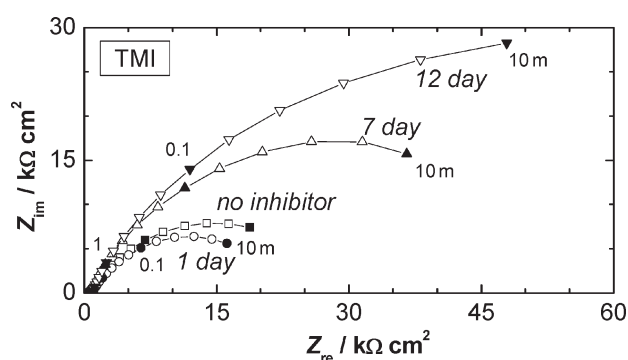


Fig. 6 – Time evolution of the impedance spectrum in the corrosion test solution containing 1 mmol L^{-1} TMI

covered with artificial patina in the corrosion test solution containing 1 mmol L^{-1} TMI. A marked decrease of the low frequency limit of the impedance, polarization resistance, can be noticed. Beyond this initial change, the polarization resistance increased continuously up to a couple of weeks. At the third week of immersion, a slight decrease of this resistance was observed. That is, the inhibiting effect of this compound improves slowly with time. A final decrease of the polarisation resistance may be explained by the roughening of the electrode surface. It is important to note that a slow increase of inhibiting effect was observed in all four cases examined in this study.

Both imidazoles examined in this study showed an inhibiting effect for Cu-8Sn-14Pb ternary bronze and Cu-6Sn binary bronze covered with artificial patina. The corrosion test in the urban

atmosphere with artists' bronze was not carried out, but the experimental method used in this work will allow a preliminary selection of inhibitors expected to be efficient towards the corrosion of bronze induced by acid rain.

Conclusions

– Artificial patina was formed electrochemically on bronzes Cu-8Sn-14Pb (B66) under constant current regulation, and Cu-6Sn under three step potential regulation in aerated sulphate/carbonate solution which simulates the formation of patina in urban atmosphere.

– The results obtained by SEM and EDS analyses have shown that patina consists of three layers of different textures on both bronzes. On the B66 bronze the outer layer (1) is turquoise blue of granular structure that consists of brochantite ($\text{Cu}_4(\text{OH})_6\text{SO}_4$) and of malachite $\text{Cu}_2(\text{CO}_3)(\text{OH})_2$. The intermediate layer (2) is rich in copper as well as oxygen. This layer may be likely constituted by the cuprite (Cu_2O) layer, characterized by reddish colour. At the inner layer (3) the copper content is low indicating the decuprification process. The tin was transformed into SnO_2 which protects copper from further oxidation. The Cu-6Sn bronze layer 1 is formed of copper-oxide and copper-sulphate. Layer 2 contains copper-sulphate crystals together with cuprite. Layer 3 consists of copper-oxide.

– The protective efficiency of two non-toxic imidazole derivatives (4-methyl-1-phenylimidazole and 4-methyl-1-(*p*-tolyl)imidazole) on bronze patinas was investigated by electrochemical impedance spectroscopy. The results of the investigation have shown that both organic compounds have protective properties on patinas on both bronzes in a medium simulating urban acid rain due to atmospheric pollution. Its protective effectiveness increases with the immersion time in the inhibitor containing the corrosion test solution.

ACKNOWLEDGEMENTS

The financial support from the Ministry of Science and Technology of the Republic of Croatia under Project 0125012 is gratefully acknowledged. The authors acknowledge EGIDE for financial support of this work through EcoNet and Cogito projects.

Symbols

c – concentration, mmol L^{-1}
 w – mass fraction, %
 j – current density, A m^{-2}
 R_e – electrolyte resistance, $\Omega \text{ m}^2$

R_f – film resistance, $\Omega \text{ m}^2$
 C_f – film capacitance, F m^{-2}
 γ – mass concentration, mmol L^{-1}
 δ – thickness, nm
 n_f – constant phase element coefficient associated with the film resistance
 R_t – charge transfer resistance, $\Omega \text{ m}^2$
 C_d – double layer capacitance, F m^{-2}
 n_d – constant phase element coefficient associated with the double layer capacitance
 R_F – faradaic resistance, $\Omega \text{ m}^2$
 C_F – faradaic capacitance, F m^{-2}
 n_F – constant phase element coefficient associated with the faradaic capacitance
 Z – impedance, $\text{k}\Omega \text{ cm}^2$

References

1. Fitzgerald, D. P., Nairn, J., Atrens, A., *Corros. Sci.* **40** (1998) 2029.
2. Robiola, L., Blengino, J.-M., Fiaud, C., *Corros. Sci.* **40** (1998) 2083.
3. Rosales, B. Vera, R., Moriema, G., *Corros. Sci.* **41** (1999) 625.
4. Rahmouni, K., Joiret, S., Robiola, L., Srhiri, A., Takenouti, H., Vivier, V., *Bulg. Chem. Communications*, **37** (2005) 26.
5. Stupnišek-Lisac, E., Cinotti, V., Reichenbach, D., *J. Appl. Electrochem.* **29** (1999) 117.
6. Gašparac, R., Martin, C. R., Stupnišek-Lisac, E., *J. Electrochem. Soc.* **147** (2000) 548.
7. Gašparac, R., Martin, C. R., Stupnišek-Lisac, E., Mandić, Z., *J. Electrochem. Soc.* **147** (2000) 991.
8. Stupnišek-Lisac, E., Galić, N., Gašparac, R., *Corrosion*, **56** (2000) 1105.
9. Stupnišek-Lisac, E., Gazivoda, A., Madžarac, M., *Electrochim. Acta*, **47** (2002) 4189.
10. Otmacić, H., Stupnišek-Lisac, E., *Electrochim. Acta*, **48** (2003) 985.
11. Otmacić, H., Telegdi, J., Papp, K., Stupnišek-Lisac, E., *J. Appl. Electrochem.* **34** (2004) 545.
12. Muresan, L., Varvara, S., Stupnišek-Lisac, E., Otmacić, H., Marušić, K., Horvat-Kurbegović, Š., Robbiola, L., Rahmouni, K., Takenouti, H., *Electrochimica Acta*, in press.
13. Serghini-Idrissi, M., Bernard, M. C., Harrif, F. Z., Joiret, S., Rahmouni, K., Srhiri, A., Takenouti, H., Vivier, V., Ziani, M., *Electrochimica Acta*, **50** (2005) 4699.
14. Robbiola, L., Pereira, N., Thawry, K., Fiaud, C., Labbé, J.-P., Decuprification phenomenon of Cu-Sn alloys in aqueous solution at nearly neutral pH condition, *METAL* 98, Ed. W. Mourey & L. Robbiola, James & James Science Publ., London (1998) 136–144.
15. Joiret, S., Rahmouni, K., Srhiri, A., Takenouti, H., Vivier, V., Eurocorr 2004, Nice September 2004, CD No 287.
16. Rahmouni, K., Robbiola, L., Srhiri, A., Takenouti, H., Ventimiglia, E., 56th Annual Meeting of the International Society of Electrochemistry, 25–30 September 2005, Busan (Korea).
17. Rahmouni, K., Ph. D. thesis, "Corrosion and protection of bronzes covered with patina: Electrochemical and spectroscopic study of the surface of archaeological artefacts and synthesis of equivalent patina on a commercial bronze", University Paris 6 and University Ibn Tofail (2005).